

PDE'S ON SURFACES – A DIFFUSE INTERFACE APPROACH

ANDREAS RÄTZ AND AXEL VOIGT

ABSTRACT. We introduce a new approach to deal with the numerical solution of partial differential equations on surfaces. Thereby we reformulate the problem on a larger domain in one higher dimension and introduce a diffuse interface region of a phase-field variable, which is defined in the whole domain. The surface of interest is now only implicitly given by the 1/2-level set of this phase-field variable. Formal matched asymptotics show the convergence of the reformulated problem to the original PDE on the surface, as the diffuse interface width shrinks to zero. The main advantage of the approach is the possibility to formulate the problem on a Cartesian grid and to reuse existing algorithms for the PDE, with only minor changes. With adaptive grid refinement the additional computational cost resulting from the higher dimension can be significantly reduced. Examples on linear diffusion and nonlinear phase separation demonstrate the wide applicability of the method.

1. INTRODUCTION

While the solution of PDEs on Cartesian grids has become a standard tool in computational science, numerical approaches to solve PDEs on surfaces is much less understood. However such problems received growing interest over the last years, due to a variety of applications. Problems of interest include image processing (e.g. [13] image the human brain), geometry (e.g. [8] deal with splines on manifolds), physiology (e.g. [7] model the liquid delivery into the lung and analyse the role of surfactants), cell-biology (e.g. [1] study domain formation in vesicles), solidification (e.g. [14] simulate ice formation on aircrafts) and gravitation (e.g. [10] simulate the bending of space and time in the surrounding of black holes).

As long as a triangulation of the surface is available such problems can be solved by parametric finite elements. See Fig. 1 for the solution of a viscous Cahn-Hilliard equation on various surfaces. The equations for the concentration u and the chemical potential μ on a surface Γ are given by

$$\begin{aligned} (1) \quad u_t &= \nu \Delta_\Gamma \mu, \\ (2) \quad \mu &= -\gamma \Delta_\Gamma u + \gamma^{-1} G'(u) + \alpha \gamma u_t \end{aligned}$$

with Δ_Γ the surface Laplacian, $G(u) = 18u^2(1-u^2)$ a double well potential, $\nu > 0$ a constant mobility, $\alpha > 0$ a constant kinetic coefficient and $\gamma > 0$

Date: November 11, 2005.

a small parameter. $u = 0$ and $u = 1$ are the two stable steady states, representing the two phases. As initial conditions we use a small zero mean perturbation of $u = 0.5$.

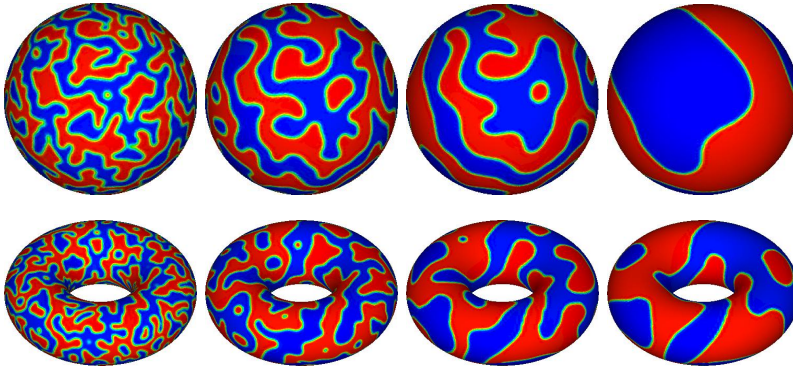


FIGURE 1. Coarsening in the viscous Cahn-Hilliard equation. Initial condition $u = 0.5$ (slightly perturbed), blue denotes $u = 0$ and red denotes $u = 1$. (top) evolution on a sphere at timesteps $t = 1.3 \cdot 10^{-3}$, $t = 4.4 \cdot 10^{-3}$, $t = 1.2 \cdot 10^{-2}$ and $t = 1.8 \cdot 10^{-1}$, (bottom) evolution on a torus at timesteps $t = 1.4 \cdot 10^{-3}$, $t = 5.4 \cdot 10^{-3}$, $t = 2.0 \cdot 10^{-2}$ and $t = 7.4 \cdot 10^{-2}$. All simulations are performed in AMDiS [18].

In a finite element software package as AMDiS [18] the same algorithms as used on a Cartesian grid can be used to solve problems on triangulated surfaces. However, well known convergence results of the numerical scheme on a Cartesian grid, can not easily be transferred to the algorithm if applied to solve the same PDE on a surface. Some of the resulting numerical analysis problems for elliptic equations are addressed in [9], but a comparable theory for parabolic problems is not available. A second problem with this approach results from the need of an appropriate surface mesh, which might not be easy to generate for complicated surfaces. Furthermore, if the surface evolves by itself, possible topological changes are hard to include in this approach.

To overcome these difficulties there have been several attempts to solve PDEs on only implicitly defined surfaces. In [2] an Eulerian method for this problem has been introduced using only a discretization on a Cartesian grid. By representing the surface as the 0-level set of a level set function ϕ defined in a domain in \mathbb{R}^d containing the surface, one can derive the Eulerian representation by replacing the surface derivatives with projections of the derivatives in the embedding Eulerian space and than solve this new representation on a Cartesian grid in a neighborhood of the surface. In particular, the surface gradient and surface Laplacian are written as

$$(3) \quad \nabla_{\Gamma} u = P \nabla \tilde{u}, \quad \text{and} \quad \Delta_{\Gamma} u = \nabla \cdot (P \nabla \tilde{u}),$$

with

$$(4) \quad P = I - \frac{\nabla\phi \otimes \nabla\phi}{|\nabla\phi|^2}.$$

Here it is assumed that \tilde{u} is a smooth function defined in an open domain containing the surface of interest, and u is the restriction of \tilde{u} to the surface. The approach has been applied to linear diffusion, anisotropic diffusion, and reaction diffusion equations [2], to the Eikonal equation [12] and more recently it has been extended to solve higher order equations [6], on surfaces of varying complexity. The viscous Cahn-Hilliard equation (1), (2) in this setting reads

$$(5) \quad \tilde{u}_t = \nu \nabla \cdot (P \nabla \tilde{\mu}),$$

$$(6) \quad \tilde{\mu} = -\gamma \nabla \cdot (P \nabla \tilde{u}) + \gamma^{-1} G'(\tilde{u}) + \alpha \gamma \tilde{u}_t.$$

The equation has been solved in [6] on the same domains as used in Fig. 1, leading to similar results. But despite the wide applicability of the method, several difficulties have been reported. Applying the method to diffusion problems results in a degenerate diffusion equation in the embedding space, as there is no diffusion in the direction perpendicular to the surface. The degeneracy problem is most severe for higher order equations and has been pointed out in [6]. A second difficulty arises by extending off initial data of the surface to the embedding domain. This has to be done with care, because the solution at the surface will be affected by these extensions. However, no matter how the extension is chosen it will change in time, and re-extension might be necessary from time to time. Furthermore the method relies on the signed-distance property of the level set function. All these difficulties probably can be overcome and have been dealt with in the level set context [17, 15]. Recently [5] improved the approach to overcome some of the difficulties. However, with no doubt, it is a powerful approach, which has already been applied to study evolution equations on varying surfaces [19].

We will present a different approach to solve PDEs on implicitly defined surfaces, which is based on a diffuse interface method, where we assume the surface to be represented by the 1/2-level set of a phase-field variable ϕ defined in a domain $\Omega \subset \mathbb{R}^d$ containing the surface Γ . The key ingredient is the function $B(\phi) = \phi^2(1-\phi)^2$, which vanishes outside the diffuse interface. Such a mobility function has been introduced in [4] to model surface diffusion within a diffuse interface approximation. Here the function $B(\phi)$ allows to rewrite rather general quasilinear elliptic and parabolic PDEs on surfaces into PDEs in \mathbb{R}^d . The viscous Cahn-Hilliard equation (1), (2) for example reads

$$(7) \quad B(\phi)\tilde{u}_t = \nu \nabla \cdot (B(\phi)\nabla \tilde{\mu}),$$

$$(8) \quad B(\phi)\tilde{\mu} = -\gamma \nabla \cdot (B(\phi)\nabla \tilde{u}) + \gamma^{-1} B(\phi)G'(\tilde{u}) + \alpha \gamma B(\phi)\tilde{u}_t$$

with \tilde{u} and $\tilde{\mu}$ smooth functions defined in $\Omega \subset \mathbb{R}^d$ approximating the solutions of (1), (2). Similar to the level set approach, only minor changes in an existing code to solve the PDE on a Cartesian grid are necessary in order to use it to solve the PDE on general surfaces. In this paper we will analyse the phase-field approach in detail. A similar approach to deal with elliptic PDEs on implicit surfaces is studied in [3].

The paper is organized as follows. In Section 2 we introduce the diffuse-interface approach, compare numerical results for a linear diffusion equation and provide a matched asymptotic analysis. In Section 3 we consider the viscous Cahn-Hilliard equation as an example of a fourth order equation and again show through matched asymptotic analysis the formal convergence of the equations (7) and (8) to the viscous Cahn-Hilliard equation on a surface (1) and (2), if the width of the diffuse interface shrinks to zero. Furthermore we show the thermodynamic consistency of the formulation. In Section 4 we describe an adaptive finite element discretization and in Section 5 we show several simulation results for the approximated viscous Cahn-Hilliard equation (7) and (8). Finally we draw conclusions.

2. DIFFUSE INTERFACE APPROXIMATION

We consider a fixed smooth surface $\Gamma \subset \mathbb{R}^d$ with $d \geq 2$ and are interested in solving PDEs on Γ .

2.1. Linear diffusion. To fix ideas we will first consider a linear diffusion equation

$$(9) \quad u_t - \Delta_\Gamma u = f \quad \text{on} \quad \Gamma \times I,$$

for $u : \Gamma \times I \rightarrow \mathbb{R}$, $I \subset \mathbb{R}$, where Δ_Γ denotes the surface Laplacian on Γ and $f : \Gamma \rightarrow \mathbb{R}$ is a smooth function. Let $\mathbf{n} : \Gamma \rightarrow S^d$ denote a normal to the surface Γ . Assuming that Γ is contained in a domain $\Omega \subset \mathbb{R}^d$ this defines an interface separating Ω in two domains Ω_{in} and Ω_{out} , where we use the convention that \mathbf{n} points from the inner domain Ω_{in} into the outer domain Ω_{out} . Then one can define an indicator function ϕ_0 being 1 in Ω_{in} and 0 in Ω_{out} . In order to introduce a diffuse interface approximation of (9) we assume that Γ can be approximated by the levelset Γ_ϵ of a phase-field function $\phi = \phi_\epsilon : \Omega \rightarrow \mathbb{R}$ with $\epsilon > 0$ obtained by smearing out the discrete function ϕ_0 on a lengthscale of order ϵ . Furthermore we assume $\phi_\epsilon(0) = 1/2$. Then a phase-field approximation for (9) can be given by

$$(10) \quad B(\phi)\tilde{u}_t - \nabla \cdot (B(\phi)\nabla\tilde{u}) = B(\phi)\tilde{f} \quad \text{on} \quad \Omega$$

for $\tilde{u} : \Omega \times I \rightarrow \mathbb{R}$ with $B(\phi) = \phi^2(1-\phi)^2$ and a sufficiently smooth extension \tilde{f} of f to the domain Ω .

2.2. Numerical results. As an example we consider the sphere $\Gamma = S^2$, which is embedded into the domain $\Omega = (-2, 2)^3$. The function

$$(11) \quad \phi = \phi(x) = \frac{1}{2} \left(1 - \tanh \left(\frac{3}{\epsilon} (|x| - 1) \right) \right)$$

serves as a phase-field approximation of Γ . Concerning the second order term in (10) we increased B by a small parameter $\delta \ll \epsilon$

$$(12) \quad B(\phi) \rightsquigarrow \delta + B(\phi).$$

On $\partial\Omega$ we assume periodic boundary conditions for \tilde{u} . For the heat equation (9) and (10), respectively, we take the right hand side function

$$f(x) = 2x_1 \quad \text{for } x \in S^2 \quad \text{and} \quad \tilde{f}(x) = \frac{2x_1}{|x|^2} \quad \text{for } x \in \Omega,$$

which yields the spherical harmonic $u(x) = x_1$ as the stationary solution of (9) and therefore a numerical benchmark to test our approach on.

Fig. 2 shows the solution of (9) and (10) with initial functions $u(x, 0) = \tilde{u}(x, 0) = 0$. Different timesteps are depicted until the stationary solution is reached.

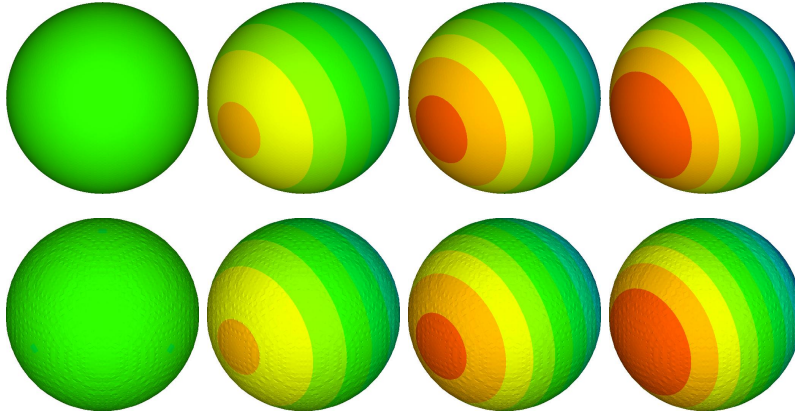


FIGURE 2. Evolution of the temperature: (top) solution u of (9), (bottom) solution $\tilde{u}|_{\Gamma}$ of (10), both at timesteps $t = 0$, $t = 0.5$, $t = 1.0$ and $t = 3.5$.

The dynamic evolution in both approaches nicely agrees and both simulations converge to the stationary solution of (9) and (10), respectively. The solutions of

$$(13) \quad -\Delta_{\Gamma} u = f$$

and

$$(14) \quad -\nabla \cdot (B(\phi)\nabla\tilde{u}) = B(\phi)\tilde{f}$$

are shown in Fig. 3. The stationary solution in both approaches can not be distinguished from each other and agree with the solution of the dynamic problem at $t = 3.5$.

Changing the extension \tilde{f} in the linear diffusion equation (10) in the numerical studies into $\tilde{f}(x) = 2x_1$ yields that the influence of the choice of the extension of parameters is negligible.

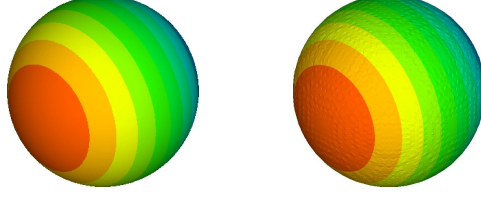


FIGURE 3. Stationary temperature: (left) solution u of (13), (right) solution $\tilde{u}|_{\Gamma}$ of (14).

2.3. Asymptotic analysis for linear diffusion equation. We now provide a matched asymptotic analysis to show the formal convergence of (10) to (9) as $\epsilon \rightarrow 0$. In the following we will drop the $\tilde{\cdot}$ in the notation, thus u denotes now also a function in Ω .

2.3.1. New coordinates. New coordinates are established in a neighborhood of the interface Γ . To this end $r = r(x; \epsilon)$ is defined as the signed distance of x from Γ_{ϵ} being positive in Ω_{out} . Furthermore let $\mathbf{X} : S \rightarrow \mathbb{R}^d$ be a parametric representation of Γ , where S is an oriented surface of dimension $d - 1$. Let $\mathbf{n} = \mathbf{n}(s; \epsilon)$, $s \in S$, denote the normal. Then we assume that for $0 < \rho \ll 1$ there exists a neighborhood

$$(15) \quad U_{\epsilon} = \{(x) \in \Omega : |r(x; \epsilon)| < \rho\}$$

of Γ_{ϵ} such that one can write $x = \mathbf{X}(s; \epsilon) + r(x; \epsilon)\mathbf{n}(s; \epsilon)$ for $x \in U_{\epsilon}$. Now one transforms u and ϕ to the new coordinate system:

$$\begin{aligned} \hat{u}(r, s, t; \epsilon) &:= u(\mathbf{X}(s; \epsilon) + r\mathbf{n}(s; \epsilon), t; \epsilon), & x \in U_{\epsilon}, \\ \hat{\phi}(r, s; \epsilon) &:= \phi(\mathbf{X}(s; \epsilon) + r\mathbf{n}(s; \epsilon); \epsilon), & x \in U_{\epsilon}. \end{aligned}$$

Furthermore a stretched variable is introduced $z := \frac{r}{\epsilon}$, and one defines

$$\begin{aligned} U(z, s, t; \epsilon) &:= \hat{u}(r, s, t; \epsilon), \\ \Phi(z, s; \epsilon) &:= \hat{\phi}(r, s; \epsilon). \end{aligned}$$

In addition the following Taylor expansion approximations for small ϵ are assumed to be valid

$$(16) \quad u(x, t; \epsilon) = u_0(x, t) + \mathcal{O}(\epsilon),$$

$$(17) \quad \hat{u}(r, s, t; \epsilon) = \hat{u}_0(r, s, t) + \mathcal{O}(\epsilon),$$

$$(18) \quad U(z, s, t; \epsilon) = U_0(z, s, t) + \epsilon U_1(z, s, t) + \epsilon^2 U_2(z, s, t) + \mathcal{O}(\epsilon^3),$$

$$(19) \quad \phi(x; \epsilon) = \phi_0(x) + \mathcal{O}(\epsilon),$$

$$(20) \quad \hat{\phi}(r, s; \epsilon) = \hat{\phi}_0(r, s) + \mathcal{O}(\epsilon),$$

$$(21) \quad \Phi(z, s; \epsilon) = \Phi_0(z, s) + \epsilon \Phi_1(z, s) + \epsilon^2 \Phi_2(z, s) + \mathcal{O}(\epsilon^3),$$

for which (16), (17) and (19), (20) are called outer expansions while (18), (21) are called inner expansion. It is assumed that these hold simultaneously

in some overlapping region and represent the same functions, which yields the matching conditions

$$(22) \quad \lim_{r \rightarrow \pm 0} \hat{u}_0(r, s, t) = \lim_{z \rightarrow \pm \infty} U_0(z, s, t),$$

$$(23) \quad \lim_{r \rightarrow \pm 0} \hat{\phi}_0(r, s) = \lim_{z \rightarrow \pm \infty} \Phi_0(z, s).$$

Let $K = K(s; \epsilon)$ denote the mean curvature of Γ . The transform of the derivatives into the new coordinates (z, s) lead

$$(24) \quad \nabla u = \epsilon^{-1} \partial_z U \mathbf{n} + \sum_{i,j=1}^2 g^{ij} \partial_{s_i} U \partial_{s_j} \mathbf{X} + \mathcal{O}(\epsilon),$$

$$(25) \quad \Delta u = \epsilon^{-2} \partial_z^2 U + \epsilon^{-1} K \partial_z U + \Delta_\Gamma U + \mathcal{O}(\epsilon),$$

where $g_{ij} := \phi_{s_i} \cdot \phi_{s_j}$ and $(g^{ij}) := (g_{ij})^{-1}$. We will need the the formula

$$(26) \quad \nabla \cdot (B(\phi) \nabla u) = \epsilon^{-2} \partial_z (B(\Phi) \partial_z U) + B(\Phi) (\epsilon^{-1} K \partial_z U + \Delta_\Gamma U) + \mathcal{O}(\epsilon).$$

Because the surface Γ is fixed, we have the time derivative

$$\partial_t u = \partial_t U.$$

2.3.2. Outer expansion. By assumption we have $\phi_0 = 1$ in Ω_{in} and $\phi_0 = 0$ in Ω_{out} and therefore $\lim_{z \rightarrow +\infty} \Phi_0 = \lim_{r \rightarrow +0} \phi_0 = 0$ as well as $\lim_{z \rightarrow -\infty} \Phi_0 = \lim_{r \rightarrow -0} \phi_0 = 1$.

2.3.3. Inner expansion. Using (26) in (10) we obtain in $\mathcal{O}(\epsilon^{-2})$

$$\partial_z (B(\Phi_0) \partial_z U_0) = 0$$

which yields $\partial_z U_0 = 0$. From this one gets in $\mathcal{O}(\epsilon^{-1})$

$$\partial_z (B(\Phi_0) \partial_z U_1) = 0$$

and therefore $\partial_z U_1 = 0$. And finally we have in $\mathcal{O}(\epsilon^0)$

$$(27) \quad B(\Phi_0) \partial_t U_0 - \partial_z (B(\Phi_0) \partial_z U_2) - B(\Phi_0) \Delta_\Gamma U_0 = B(\Phi_0) F_0,$$

where we have used $\partial_s \Phi_0 = 0$. Furthermore one easily verifies that $\partial_z F_0 = 0$, and integration of (27) yields

$$\int_{-\infty}^{+\infty} B(\Phi_0) dz \partial_t U_0 - \int_{-\infty}^{+\infty} B(\Phi_0) dz \Delta_\Gamma U_0 = \int_{-\infty}^{+\infty} B(\Phi_0) dz F_0.$$

Dividing this equation by $\int_{-\infty}^{+\infty} B(\Phi_0) dz$ we end up with

$$\partial_t U_0 - \Delta_\Gamma U_0 = F_0.$$

Thus with $F_0 = f$ and $\lim_{z \rightarrow \pm \infty} U_0 = \lim_{r \rightarrow \pm 0} u_0 = u_0|_\Gamma$ we have shown the formal convergence to the linear diffusion equation (9) on the surface Γ .

2.4. More general parabolic equations. After this promising result we want to generalize the equation and summarize the ingredients for the diffuse-interface approach to solve problems on surfaces. Denoting the tangent space of Γ in $x \in \Gamma$ with $T_x\Gamma$ a more general second order PDE on a surface Γ reads

$$u_t - \nabla_\Gamma \cdot (A \nabla_\Gamma u) + b \cdot \nabla_\Gamma u + cu = f$$

with a positive definite symmetric endomorphism $A = A(u, \nabla_\Gamma u, x, t) : T_x\Gamma \rightarrow T_x\Gamma$, $b = b(u, \nabla_\Gamma u, x, t) : T_x\Gamma \rightarrow \mathbb{R}$, $c = c(u, \nabla_\Gamma u, x, t) \in \mathbb{R}$ and $f = f(x, t)$. Here $A(\cdot)$, $b(\cdot)$, $c(\cdot)$ and $f(\cdot)$ are assumed to be sufficiently smooth. To transform it into a PDE in Ω we need to extend all parameters in a sufficiently smooth manner. The diffuse interface approximation then reads

$$B(\phi)\tilde{u}_t - \nabla \cdot (B(\phi)\tilde{A}\nabla\tilde{u}) + B(\phi)\tilde{b} \cdot \nabla\tilde{u} + B(\phi)\tilde{c}\tilde{u} = B(\phi)\tilde{f},$$

where \tilde{A} is a positive definite extension of the endomorphism A to normal vectors and the extension \tilde{b} of b to normal vectors can be arbitrarily chosen. The matched asymptotic analysis can be done along the same lines as for the linear problem.

3. THE VISCOUS CAHN-HILLIARD EQUATION

We will now return to the viscous Cahn-Hilliard equation on a surface, whose diffuse interface approximation is repeated here again for consistency

$$(28) \quad B(\phi)u_t = \nu \nabla \cdot (B(\phi)\nabla\mu),$$

$$(29) \quad B(\phi)\mu = -\gamma \nabla \cdot (B(\phi)\nabla u) + \gamma^{-1}B(\phi)G'(u) + \alpha\gamma B(\phi)u_t.$$

3.1. Thermodynamic consistency. The diffuse-interface approximation to the viscous Cahn-Hilliard equation on a surface (28) and (29) has the properties of a gradient flow of the following energy

$$(30) \quad E(u) = \int_\Omega \gamma^{-1}B(\phi)G(u) + \gamma \frac{1}{2}B(\phi)|\nabla u|^2.$$

The time derivative can thus be computed as

$$\begin{aligned} \partial_t E(u) &= \int_\Omega \gamma^{-1}B(\phi)G'(u)\partial_t u + \gamma B(\phi)\nabla u \cdot \nabla u_t \\ &= \int_\Omega (\gamma^{-1}B(\phi)G'(u) - \gamma \nabla \cdot (B(\phi)\nabla u))u_t \\ &= \int_\Omega (B(\phi)\mu - \alpha\gamma B(\phi)u_t)u_t \\ &= \int_\Omega \mu\nu \nabla \cdot (B(\phi)\nabla\mu) - \alpha\gamma B(\phi)(u_t)^2 \\ &= \int_\Omega -\nu B(\phi)(\nabla\mu)^2 - \alpha\gamma B(\phi)(u_t)^2 \leq 0, \end{aligned}$$

where eq. (7) and (8) have been used. Thus the dissipation inequality holds for the introduced diffuse interface approximation, which shows its thermodynamic consistency. The same holds for the two limiting cases:

(1) the Cahn-Hilliard equation, which is obtained as $\alpha \rightarrow 0$

$$\begin{aligned} B(\phi)u_t &= \nu \nabla \cdot (B(\phi) \nabla \mu), \\ B(\phi)\mu &= -\gamma \nabla \cdot (B(\phi) \nabla u) + \gamma^{-1} B(\phi) G'(u), \end{aligned}$$

and

(2) the Allen-Cahn equation, which can be obtained as $\nu \rightarrow \infty$

$$\alpha \gamma B(\phi)u_t = \gamma \nabla \cdot (B(\phi) \nabla u) - \gamma^{-1} B(\phi) G'(u).$$

It remains to show the convergence of the diffuse interface approximation to the viscous Cahn-Hilliard equation on a surface to (1) and (2) as $\epsilon \rightarrow 0$.

3.2. Asymptotic analysis for viscous Cahn-Hilliard equation. Note that we have two distinguished interface parameters: γ the intrinsic diffuse interface width in the viscous Cahn-Hilliard equation on the surface Γ , and ϵ the diffuse interface width of the phase-field approximation in Ω . Here we consider the limit $\epsilon \rightarrow 0$.

3.2.1. New coordinates. Extending the notation in Section 2.3 by introducing

$$\hat{\mu}(r, s, t; \epsilon) := \mu(\mathbf{X}(s; \epsilon) + r\mathbf{n}(s; \epsilon), t; \epsilon), \quad x \in U_\epsilon$$

and

$$M(z, s, t; \epsilon) := \hat{\mu}(r, s, t; \epsilon)$$

and assuming the Taylor expansion approximations for small ϵ to be valid

$$(31) \quad \mu(x, t; \epsilon) = \mu_0(x, t) + \mathcal{O}(\epsilon),$$

$$(32) \quad \hat{\mu}(r, s, t; \epsilon) = \hat{\mu}_0(r, s, t) + \mathcal{O}(\epsilon),$$

$$(33) \quad M(z, s, t; \epsilon) = M_0(z, s, t) + \epsilon M_1(z, s, t) + \epsilon^2 M_2(z, s, t) + \mathcal{O}(\epsilon^3)$$

and that these hold simultaneously in some overlapping region and represent the same functions, we obtain the additional matching condition

$$(34) \quad \lim_{r \rightarrow \pm 0} \hat{\mu}_0(r, s, t) = \lim_{z \rightarrow \pm \infty} M_0(z, s, t).$$

3.2.2. Outer expansion. See the case of the linear diffusion equation.

3.2.3. Inner expansion. Using the inner expansions in (28) and (29) we obtain in $\mathcal{O}(\epsilon^{-2})$

$$\begin{aligned} \partial_z(B(\Phi_0)\partial_z M_0) &= 0, \\ \partial_z(B(\Phi_0)\partial_z U_0) &= 0 \end{aligned}$$

which yield $\partial_z M_0 = 0$ and $\partial_z U_0 = 0$. From these one gets in $\mathcal{O}(\epsilon^{-1})$

$$\begin{aligned}\partial_z(B(\Phi_0)\partial_z M_1) &= 0, \\ \partial_z(B(\Phi_0)\partial_z U_1) &= 0\end{aligned}$$

and therefore $\partial_z M_1 = 0$ and $\partial_z U_1 = 0$. And finally we have in $\mathcal{O}(\epsilon^0)$

$$\begin{aligned}B(\Phi_0)\partial_t U_0 &= \nu(\partial_z(B(\Phi_0)\partial_z M_2) + B(\Phi_0)\Delta_\Gamma M_0), \\ B(\Phi_0)M_0 &= -\gamma(\partial_z(B(\Phi_0)\partial_z U_2) + B(\Phi_0)\Delta_\Gamma U_0) \\ &\quad + \gamma^{-1}B(\Phi_0)G'(U_0) + \alpha\gamma B(\Phi_0)\partial_t U_0\end{aligned}$$

where we have used $\partial_s \Phi_0 = 0$. Integration of both equations yields

$$\begin{aligned}\int_{-\infty}^{+\infty} B(\Phi_0) dz \partial_t U_0 &= \nu \int_{-\infty}^{+\infty} B(\Phi_0) dz \Delta_\Gamma M_0, \\ \int_{-\infty}^{+\infty} B(\Phi_0) dz M_0 &= - \int_{-\infty}^{+\infty} B(\Phi_0) dz \gamma \Delta_\Gamma U_0 \\ &\quad + \int_{-\infty}^{+\infty} B(\Phi_0) dz \gamma^{-1} G'(U_0) + \int_{-\infty}^{+\infty} B(\Phi_0) dz \alpha \gamma \partial_t U_0.\end{aligned}$$

Dividing these equations by $\int_{-\infty}^{+\infty} B(\Phi_0) dz$ we end up with

$$\begin{aligned}\partial_t U_0 &= \nu \Delta_\Gamma M_0, \\ M_0 &= -\gamma \Delta_\Gamma U_0 + \gamma^{-1} G'(U_0) + \alpha \gamma \partial_t U_0,\end{aligned}$$

on Γ , which is by matching conditions (22) and (34) the viscous Cahn-Hilliard equation (1) and (2) for $u_0|_\Gamma$ and $\mu_0|_\Gamma$.

4. NUMERICAL APPROACH

We adapt the numerical approach used in [16] to solve a viscous Cahn-Hilliard equation with a degenerate mobility function.

4.1. Finite element discretization. The time interval is split by discrete time instants $0 = t_0 < t_1 < \dots$, from which one gets the time steps $\Delta t_m := t_{m+1} - t_m$. The derivative of the doublewell potential is linearized by

$$\begin{aligned}G'(u^{(m+1)}) &\approx G'(u^{(m)}) + G''(u^{(m)})(u^{(m+1)} - u^{(m)}) \\ &= G''(u^{(m)})u^{(m+1)} + G'(u^{(m)}) - G''(u^{(m)})u^{(m)}.\end{aligned}$$

Using this time discretization one ends up with the weak formulation

$$\begin{aligned}
& \frac{1}{\Delta t_m} \int_{\Omega} B(\phi) u^{(m+1)} \psi + \nu \int_{\Omega} B(\phi) \nabla \mu^{(m+1)} \cdot \nabla \psi \\
&= \frac{1}{\Delta t_m} \int_{\Omega} B(\phi) u^{(m)} \psi, \\
& - \int_{\Omega} B(\phi) \mu^{(m+1)} \psi + \gamma \int_{\Omega} B(\phi) \nabla u^{(m+1)} \cdot \nabla \psi \\
& \quad + \gamma^{-1} \int_{\Omega} B(\phi) G''(u^{(m)}) u^{(m+1)} \psi + \frac{\gamma \alpha}{\Delta t_m} \int_{\Omega} B(\phi) u^{(m+1)} \psi \\
&= \frac{\gamma \alpha}{\Delta t_m} \int_{\Omega} B(\phi) u^{(m)} \psi - \gamma^{-1} \int_{\Omega} B(\phi) (G'(u^{(m)}) - G''(u^{(m)}) u^{(m)}) \psi
\end{aligned}$$

for all $\psi \in X^d := \{\psi \in H^1(\Omega) : \psi|_{\partial\Omega} \text{ periodic}\}$. To discretize in space, let \mathcal{T}_h be a conforming triangulation of Ω . Define the finite element space of globally continuous, piecewise linear elements $\mathbb{V}_h = \{v_h \in X^d : v_h|_T \in \mathbb{P}^1 \ \forall T \in \mathcal{T}_h\}$. The space discretization now reads: Find $u_h^{(m+1)}, \mu_h^{(m+1)} \in \mathbb{V}_h$ such that

$$\begin{aligned}
& \frac{1}{\Delta t_m} \int_{\Omega} B(\phi) u_h^{(m+1)} \psi + \nu \int_{\Omega} B(\phi) \nabla \mu_h^{(m+1)} \cdot \nabla \psi \\
&= \frac{1}{\Delta t_m} \int_{\Omega} B(\phi) u_h^{(m)} \psi, \\
& - \int_{\Omega} B(\phi) \mu_h^{(m+1)} \psi + \gamma \int_{\Omega} B(\phi) \nabla u_h^{(m+1)} \cdot \nabla \psi \\
& \quad + \gamma^{-1} \int_{\Omega} B(\phi) G''(u_h^{(m)}) u_h^{(m+1)} \psi + \frac{\gamma \alpha}{\Delta t_m} \int_{\Omega} B(\phi) u_h^{(m+1)} \psi \\
&= \frac{\gamma \alpha}{\Delta t_m} \int_{\Omega} B(\phi) u_h^{(m)} \psi - \gamma^{-1} \int_{\Omega} B(\phi) (G'(u_h^{(m)}) - G''(u_h^{(m)}) u_h^{(m)}) \psi
\end{aligned}$$

for all $\psi \in \mathbb{V}_h$. These lead to a linear system of equations for $U^{(m+1)}$ and $W^{(m+1)}$, with $u_h^{(m+1)} = \sum U_i^{(m+1)} \psi_i$ and $\mu_h^{(m+1)} = \sum W_i^{(m+1)} \psi_i$

$$\begin{aligned}
& \frac{1}{\Delta t_m} \mathbf{M} U^{(m+1)} + \nu \mathbf{A} W^{(m+1)} = \frac{1}{\Delta t_m} \mathbf{M} U^{(m)}, \\
& -\mathbf{M} W^{(m+1)} + \gamma \mathbf{A} U^{(m+1)} + \gamma^{-1} \mathbf{G}^i U^{(m+1)} + \frac{\gamma \alpha}{\Delta t_m} \mathbf{M} U^{(m+1)} = \frac{\gamma \alpha}{\Delta t_m} \mathbf{M} U^{(m)} \\
& \quad -\gamma^{-1} \mathbf{G}^e
\end{aligned}$$

with

$$\begin{aligned}
\mathbf{M} &= (M_{ij}) & M_{ij} &= (B(\phi) \psi_i, \psi_j)_{\Omega}, \\
\mathbf{A} &= (A_{ij}) & A_{ij} &= (B(\phi) \nabla \psi_i, \nabla \psi_j)_{\Omega}, \\
\mathbf{G}^i &= (G_{ij}^i) & G_{ij}^i &= (B(\phi) G''(u_h^{(m)}) \psi_i, \psi_j)_{\Omega}, \\
\mathbf{G}^e &= (G_i^e) & G_i^e &= (B(\phi) (G'(u_h^{(m)}) - G''(u_h^{(m)})) u_h^{(m)}, \psi_i)_{\Omega},
\end{aligned}$$

where $(\cdot, \cdot)_\Omega$ denotes the L^2 scalar product. Thus, written in block-matrix-form the linear system

$$\begin{pmatrix} \nu \mathbf{A} & \frac{1}{\Delta t_m} \mathbf{M} \\ -\mathbf{M} & \gamma \mathbf{A} + \gamma^{-1} \mathbf{G}^i + \frac{\gamma \alpha}{\Delta t_m} \mathbf{M} \end{pmatrix} \begin{pmatrix} W^{(m+1)} \\ U^{(m+1)} \end{pmatrix} = \begin{pmatrix} \frac{1}{\Delta t_m} \mathbf{M} U^{(m)} \\ \frac{\gamma \alpha}{\Delta t_m} \mathbf{M} U^{(m)} + \gamma^{-1} \mathbf{G}^e \end{pmatrix}$$

has to be solved in every timestep. The system is not symmetric and is iteratively solved by a stabilized bi-conjugate gradient method (BiCGStab).

4.2. Adaptivity. Adaptive mesh refinement is a key ingredient to an efficient algorithm for this class of problems, because it helps to reduce the amount of additional work the extra dimension requires. Outside the diffuse interface region the mesh can be rather coarse, without influencing the solution on the surface. As a first approach towards an adaptive scheme we therefore choose a jump residual as an indicator, to refine the mesh. An error estimate for the viscous Cahn-Hilliard equation itself, accounting for different grid refinements within the diffuse interface, has not been used yet. Thus the grid is homogeneous within the diffuse interface, with a grid size $h \approx \epsilon/5$ and $\epsilon = 2\gamma = 0.1$. Fig. 4 shows the grid used in the computations.

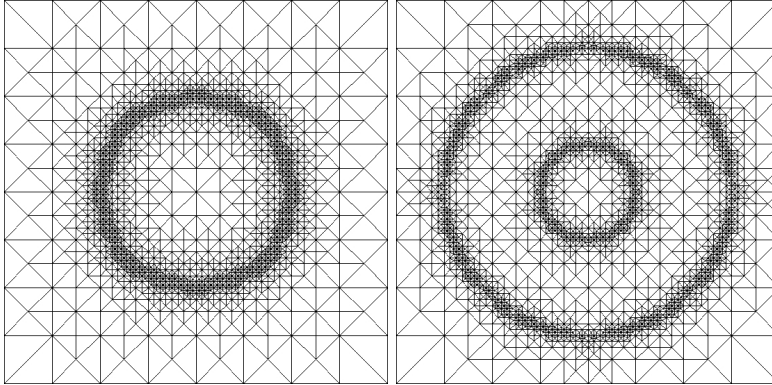


FIGURE 4. Adaptively refined mesh (cross section): (left) sphere, (right) torus.

Furthermore a simple strategy of time adaptivity is used, where the timestep is inversely proportional to the maximum of the normal velocity of the Cahn-Hilliard interface leading to timesteps $\Delta t_m \in [10^{-5}, 10^{-4}]$. This means that the timesteps are increased by two orders of magnitude compared to a restriction of order $h^4 \approx 1.6 \cdot 10^{-7}$ an explicit scheme would require.

5. SIMULATION RESULTS

The method is implemented in AMDiS [18]. As in the simulations shown in Fig. 1 we use as initial conditions a small zero mean perturbation of $u = 0.5$. Again the sphere is given as the level set $\phi = 1/2$ of the function

(11), and in the case of the torus we have used a slightly more complicated tanh-construction than for the sphere. Furthermore we regularize the second order terms in (28), (29) in the same way as in the case of the diffusion equation (see (12)). Fig. 5 shows the evolution of the diffuse interface approximation of the viscous Cahn-Hilliard equation on a surface. The figure shows the value of u on the 1/2-level set of the phase-field variable ϕ . The simulation results agree very well with the results shown in Fig. 1 at corresponding timesteps, where in all cases we have used the parameters $\alpha = \nu = 1.0$.

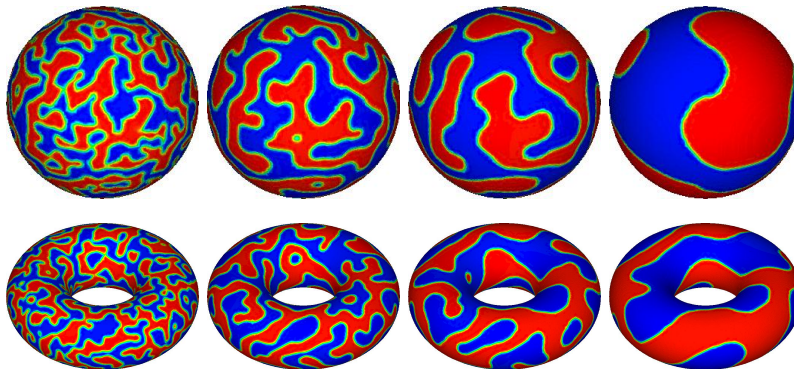


FIGURE 5. Coarsening in the viscous Cahn-Hilliard equation (diffuse interface approximation). Blue denotes $u = 0$ and red denotes $u = 1$. (top) evolution on a sphere at timesteps $t = 1.3 \cdot 10^{-3}$, $t = 4.4 \cdot 10^{-3}$, $t = 1.2 \cdot 10^{-2}$ and $t = 1.8 \cdot 10^{-1}$, (bottom) evolution on a torus at timesteps $t = 1.4 \cdot 10^{-3}$, $t = 5.4 \cdot 10^{-3}$, $t = 2.0 \cdot 10^{-2}$ and $t = 7.4 \cdot 10^{-2}$.

The phase-field variable ϕ is in both cases constructed by hand. For more complex geometries this is unfeasible. In these cases an indicator function $I(x)$, with $I(x) = 0$ on one side of the surface Γ and $I(x) = 1$ on the other side, can be used as an initial function for ϕ . To construct an appropriate phase-field variable to represent the surface, a few time steps of

$$\begin{aligned}\phi_t &= \epsilon^{-1} \nabla \cdot (B(\phi) \nabla \mu), \\ \mu &= -\epsilon \Delta \phi + \epsilon^{-1} G'(\phi).\end{aligned}$$

can be performed. The equation will smear out the initial function at the beginning, without changing the 1/2-level set too much.

6. CONCLUSION

We have presented a new approach to solve PDEs on surfaces. The problem is reformulated on a larger domain in one higher dimension and is based on a diffuse interface approximation. The surface is the 1/2-level set of a phase-field variable. Formal matched asymptotics show the convergence

to the PDE on the surface as the diffuse interface width goes to zero. The method is applied to a linear diffusion problem, which serves as a benchmark and to a nonlinear fourth-order problem to demonstrate its applicability for a general class of PDEs. The approach is here restricted to stationary surfaces, however the way to include motion of the surface is straight forward and is under investigation [11]. The introduced diffuse interface approach has the same advantages as the level set method to solve an Eulerian representation of the PDE on the surface. Especially with the use of an adaptive grid, it can compete with the common narrow-band approach in the level set method. Furthermore, due to the decoupling of the surface representation through the phase-field variable ϕ and the evolution equation, the method is much more insensitive on the way data are extended away from the surface, and the initial properties of ϕ remain throughout the simulation.

Acknowledgment: We would like to thank Martin Burger and John Lowengrub for stimulating discussions. Financial support is acknowledged by DFG through SPP 1095 (grant Vo 899/3-1) and EU through FP6 (grant NMP-STRP 06447 MagDot).

REFERENCES

- [1] G.S. Ayton, J.L. McWhirter, P. McMurty, and G.A. Voth. Coupling field theory with continuum mechanics: A simulation of domain formation in giant unilamellar vesicles. *Biophys. J.*, 88:3855–3869, 2005.
- [2] M. Bertalmio, L.-T. Cheng, S. Osher, and G. Sapiro. Variational problems and partial differential equations on implicit surfaces. *J. Comput. Phys.*, 174(2):759–780, 2001.
- [3] M. Burger. Finite element approximation of elliptic partial differential equations on implicit surfaces. *Comput. Vis. Sci.*, in review.
- [4] J. Cahn, C.M. Elliott, and A. Novick-Cohen. The Cahn-Hilliard equation with a concentration dependent mobility. Motion by minus the Laplacian of the mean curvature. *Euro. J. Appl. Math.*, 7:287–301, 1996.
- [5] J.B. Greer. An improvement of a recent Eulerian method for solving PDEs on general geometries. *J. Sci. Comput.*, in print.
- [6] J.B. Greer, A.L. Bertozzi, and G. Sapiro. Fourth order partial differential equations on general geometries. *J. Comput. Phys.*, in review.
- [7] D. Halpern, O.E. Jenson, and J.B. Grotberg. A theoretical study of surfactant and liquid delivery into the lung. *J. Appl. Physiology*, 85:333–352, 1998.
- [8] M. Hofer and H. Pottmann. Energy-minimizing splines in manifolds. *ACM Trans. Graphics*, 23:284–293, 2004.
- [9] M.J. Holst. Adaptive numerical treatment of elliptic systems on manifolds. *Adv. Comput. Math.*, 15:139–191, 2001.
- [10] M.J. Holst and D. Bernstein. Adaptive finite element solution of the initial value problem in general relativity i. algorithms. in preparation.
- [11] J.S. Kim, J.S. Lowengrub, A. Rätz, and A. Voigt. Coexisting fluid domains in biomembrane models. in preparation.
- [12] F. Memoli and G. Sapiro. Fast computation of weighted distance functions and geodesics on implicit hyper-surfaces. *J. Comput. Phys.*, 173(2):730–764, 2001.
- [13] F. Memoli, G. Sapiro, and P. Thompson. Implicit brain imaging. *Human Brain Mapping*, 23:179–188, 2004.

- [14] T.G. Myers and J.P.F. Charpin. A mathematical model for atmospheric ice accretion and water flow on a cold surface. *Int. J. Heat Mass Trans.*, 47:5483–5500, 2004.
- [15] S. Osher and R. Fedkiw. *Level set methods and dynamic implicit surfaces*. Springer-Verlag, 2003.
- [16] A. Rätz, A. Ribalta, and A. Voigt. Surface evolution of elastically stressed films under deposition by a diffuse interface model. *J. Comput. Phys.*, in print.
- [17] J.A. Sethian. *Level set methods and fast marching method. Evolving interfaces in computational geometry, fluid mechanics, computer vision, and materials sciences*. Cambridge University Press, 1999.
- [18] S. Vey and A. Voigt. AMDiS - Adaptive Multidimensional Simulations. *Comp. Vis. Sci.*, in review.
- [19] J. Xu and H.K. Zhao. An Eulerian formulation for solving partial differential equations along a moving interface. *J. Sci. Comput.*, 19:573–594, 2003.

ANDREAS RÄTZ, CRYSTAL GROWTH GROUP, RESEARCH CENTER CAESAR, LUDWIG-ERHARD-ALLEE 2, 53175 BONN, GERMANY

E-mail address: `raetz@caesar.de`

AXEL VOIGT, CRYSTAL GROWTH GROUP, RESEARCH CENTER CAESAR, LUDWIG-ERHARD-ALLEE 2, 53175 BONN, GERMANY, AND, IPAM, UNIVERSITY OF CALIFORNIA, LOS ANGELES, LOS ANGELES, CA 90095-7121, USA

E-mail address: `voigt@caesar.de`